The Astrophysical Journal, 680:1508–1515, 2008 June 20

THE EFFECT OF MAGNETIC RECONNECTION AND WRITHING IN A PARTIAL FILAMENT ERUPTION

Rui Liu,[1] Holly R. Gilbert,[1] David Alexander,[1] and Yingna Su[2,3]

Received 2007 December 6; accepted 2008 January 29

ABSTRACT

We present observations from 2007 March 2 of a partial filament eruption characterized by two distinct phases of writhing motions: a quasi-static, slowly evolving phase followed by a rapid kinking phase showing a bifurcation of the filament. The quasi-static kinking motions are observed before there is any heating or flaring evident in EUV or soft X-ray (SXR) observations. As the writhe of the filament develops, a sigmoid becomes sharply defined in the SXR. Prior to eruption onset, the sigmoid in the EUV appears to be composed of two separate looplike structures, which are discontinuous at the projected location where the sigmoid crosses the filament. Coincident with the onset of the eruption and the production of a *GOES* class B2 flare, the original "two-loop" EUV sigmoid is now observed as a single continuous structure lying above the filament, signifying the presence of magnetic reconnection and the associated dissipative heating of field lines above the filament. During the eruption, the escaping portion of the filament rotates quickly and erupts together with the expanding arched sigmoid. The portion of the filament that is left behind develops into an inverse S–shaped configuration. The separation of the filament, the EUV brightening at the separation location, and the surviving sigmoidal structure are all signatures of magnetic reconnection occurring within the body of the original filament. Other features of the same event reported by Sterling and coworkers, e.g., the flux cancellation at the polarity inversion line prior to the eruption and the SXR compact loop formed underneath the erupting sigmoid during the eruption, indicate that magnetic reconnection also occurred in the sheared core field beneath the filament. These results suggest that a combination of the kinking motions and internal tether-cutting are responsible for the initiation of the eruption.

Subject headings: Sun: corona — Sun: filaments

Online material: color figures, mpeg animations

1. INTRODUCTION

Eruptive solar filaments that display a helically deformed axis are often regarded as the "fingerprint" of the MHD helical kink instability (e.g., Rust & LaBonte 2005). A magnetic flux rope becomes kink-unstable if the twist of the field, a measure of the number of windings of field lines around the axis of the rope, exceeds a critical value (e.g., Fan 2005; Török & Kliem 2005). The axis then exhibits writhing motions, and the twist is converted to the writhe of the field, a measure of the twist of the axis itself, due to the conservation of magnetic helicity in the highly conducting corona (Berger 1998). Consequently, the flux rope may totally or partially erupt (e.g., Williams et al. 2005; Romano et al. 2003; Liu et al. 2007), or it may be confined in the lower corona (e.g., Alexander et al. 2006). Quantifying the amount of kinking, i.e., the conversion of twist to writhe, in observations is challenging due to projection effects. With two-dimensional observations, even when the filament is viewed directly from above, only the rotation of the axis can be measured as the angle between the orientations of the central portion of the filament and the polarity inversion line along which the filament is originally aligned. This is effectively a measurement of the nonlocal writhe, as defined by Berger & Prior (2006), with the local writhe remaining observationally undetermined due to the limitations of line-of-sight integrated observations.

A distinctive set of structures linked to filaments are sigmoids, which are forward or inverse S-shaped hot coronal loops that are frequently observed in soft X-ray (SXR) emission and are reminiscent of twisted or sheared field lines (Rust & Kumar 1994, 1996; Titov & Démoulin 1999). Sigmoids often brighten prior to or during the impulsive stage of coronal eruptions. Typically they transform into arcades or cusped loops as the eruption progresses (e.g., Sterling et al. 2000; Moore et al. 2001; Pevtsov 2002; Gibson et al. 2002), but the associated active regions can exhibit sigmoidal structures again within a matter of hours after the eruption. The central portion of such transient sigmoids is approximately aligned with the polarity inversion line along which a filament often lies. Filaments were observed in 124 (91%) of the 136 sigmoid active regions in a study by Pevtsov (2002). Intriguingly, some filaments in sigmoidal regions appear to be largely unperturbed by the sigmoid-to-arcade transformation and the consequent coronal mass ejections (CMEs; Pevtsov 2002; Gibson et al. 2002). One of the earliest models that addresses the relationship between the SXR sigmoid and Hα filament is the tether-cutting model (Moore & LaBonte 1980; Moore et al. 2001). In this model the sigmoid is composed of two oppositely curved elbows crossing over the polarity inversion line, and a filament is supported by the dips of sheared core field between the elbow arms (see Fig. 1*a* in Moore et al. 2001). At the eruption onset, the two crossed arms reconnect to form two sets of field lines, one set escaping upward from the reconnection site and the other moving downward (see Fig. 1*b* in Moore et al. 2001). The upward-directed field lines form a rising twisted flux rope that carries the filament with it, while the downward-directed field lines form low-lying compact loops. Titov & Démoulin (1999), however, suggested that the transient sigmoid brightening is a manifestation of the formation of a strong current layer, stimulated by an ideal MHD instability, such as the kink instability (Kliem et al. 2004; Gibson et al. 2004), or the catastrophe of a flux rope.

Filaments are often observed to partially erupt or immediately reform after the eruption (e.g., Gilbert et al. 2000, 2001; Liu et al.

[1] Department of Physics and Astronomy, Rice University, Houston, TX 77005; rliu@rice.edu.

[2] Harvard-Smithsonian Center for Astrophysics, Cambridge, MA 02138.

[3] Purple Mountain Observatory, Nanjing; and Graduate University of Chinese Academy of Sciences, China.

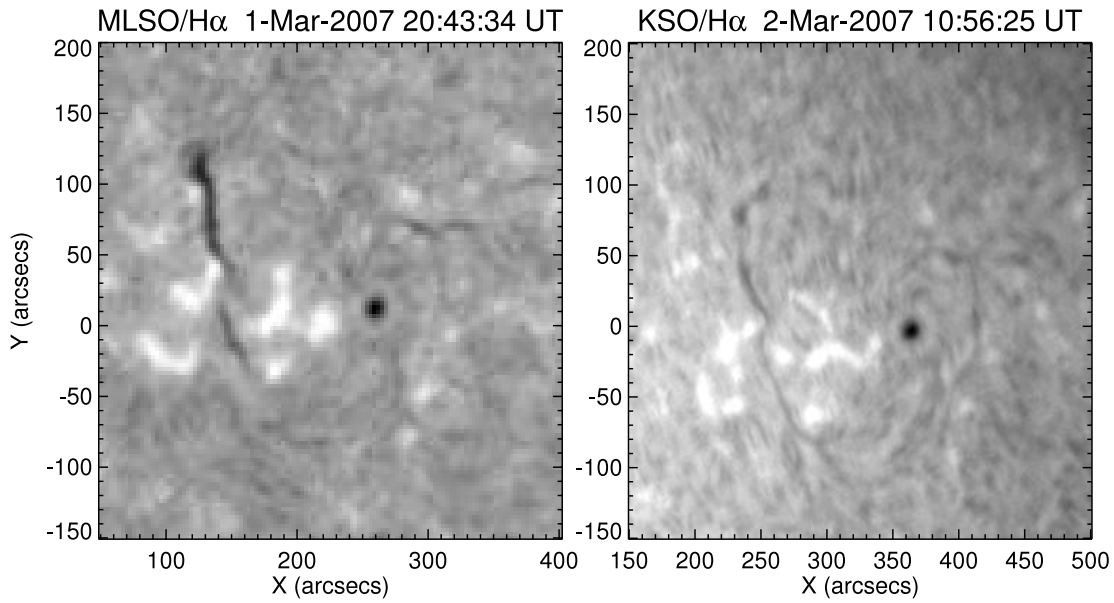

FIG. 1.—Active region in which the partial eruption occurred, shown in Hα.

2007). Gilbert et al. (2001) suggested that within a flux rope configuration where filament mass is supported by the concave-upward fields, the occurrence and location of magnetic reconnection serves to create a range of different topological changes with implications for the full, partial, or failed eruption of the filament. When reconnection occurs within the filament, it causes a part of the filament to separate and erupt with the CME, while the remainder of the filament becomes magnetically disconnected from the CME and drops back toward the surface (see Fig. 3 in Gilbert et al. 2001). Recently Gibson & Fan (2006a) demonstrated in three-dimensional (3D) simulations the partial eruption scenario in which a kinking flux rope is separated into two by multiple reconnections at internal current sheets formed as the flux rope writhes and expands upward. The transient sigmoid within their framework is the manifestation of the helical field lines heated by the dissipation of the current sheets along a topological surface that separates the twisted fields from the surrounding untwisted fields, as predicted by Titov & Démoulin (1999).

In this paper we present observations of a partial filament eruption event in which the detailed evolution of the EUV sigmoid and the separation of the filament shed some light on the role of the kink instability and associated magnetic reconnection in coronal eruptions. Recently Sterling et al. (2007) studied the same event and made a thorough analysis of the evolution of the photospheric magnetic fields and the evolution of the SXR sigmoid. We, however, provide a different perspective on this event by focusing on several distinctive features in the EUV data, leading to a somewhat different but more comprehensive interpretation. We will present the observations and data analysis in § 2 and discuss the results in § 3.

2. OBSERVATIONS AND ANALYSIS

The partial filament eruption occurred close to the solar disk center in NOAA active region (AR) 0944 at about 05:00 UT on 2007 March 2. Our predominant data sources are EUV images obtained by the *Transition Region and Coronal Explorer* (*TRACE*; Handy et al. 1999) and soft X-ray images obtained by the *Hinode* X-Ray Telescope (XRT; Golub et al. 2007). The XRT images used in this paper have an overall size of 512 pixels $\times$ 512 pixels, with a typical temporal cadence of 2 minutes and a pixel size of 1.032″. Images are taken with the Ti-poly filter, which has a broad temperature response function with a relatively flat peak at about $10^{6.9}$ MK. The exposure time of images adopted is around 2 s prior to the flare, but less than 1 s during the flare, to avoid saturation. The pre-eruption activity of the filament was recorded by the 171 Å filter of the EUV imager (EUVI; Wuelser et al. 2004) on board the *Solar Terrestrial Relations Observatory* (*STEREO*), with a temporal cadence of 2.5 minutes and a pixel resolution of 1.59″. Details of the observations are explained below.

2.1. *Quasi-static Kinking*

Figure 1 shows NOAA AR 0944 several hours before and after the eruption in Hα, using images obtained at Mauna Loa Solar Observatory (MLSO) and at Kanzelhöhe Solar Observatory (KSO). Observed in absorption as dark features, the filament is oriented primarily north-south, located to the east of a sunspot. About 5 hr after the eruption (Fig. 1, *right*), the filament has reformed, but a considerable portion of the filament mass has been lost. It is difficult to verify if the filament eruption is associated with a CME, as this relatively small eruption occurred close to the disk center, and indeed no CME was reported by either *SOHO* LASCO (data gap from 02:36 to 13:12 UT) or *STEREO* COR1 within hours after the eruption occurred. However, the filament mass loss and the separation of the filament with the escaping part leaving the *TRACE* field of view (§ 2.3) indicate the occurrence of a partial filament eruption (Gilbert et al. 2007). Sterling et al. (2007) reported that for at least 6 hr prior to the eruption, the Solar Optical Telescope (SOT) on board *Hinode* observed opposite magnetic elements flowing together and canceling each other at the polarity inversion line along which the filament was aligned.

Figure 2*a* shows the filament as a dark, elongated structure in the *STEREO* EUVI Fe IX/X 171 Å filter as it absorbs the optically thin EUV emission underneath. By concentrating on the filament region (see the rectangle in Fig. 2*a*), it can be seen that the filament slowly rotates counterclockwise, with its northern end relatively fixed and the southern end moving westward (see Fig. 2*b*). By 04:34 UT, the rotation angle about the northern end is approximately 17°. A bright ribbon-like structure crossing the filament can be seen in the same panel. The ribbon-like structure developed into the northern "elbow" of a transient sigmoid in the later

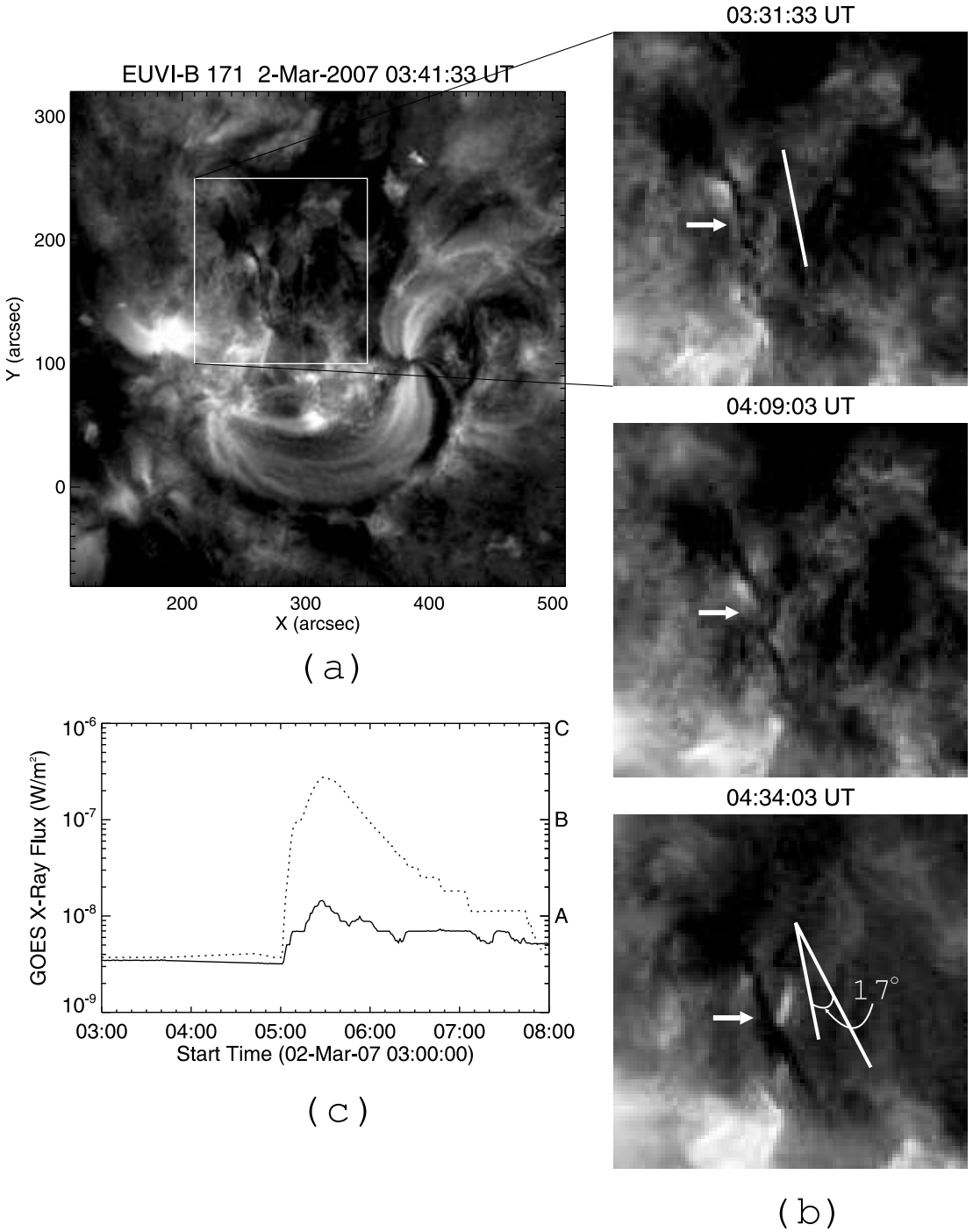

FIG. 2.—Evolution of the filament in its earlier quiescent stage. (*a*) The active region of interest, observed with *STEREO-B* EUVI at 171 Å about 1.5 hr prior to the dynamic stage of the eruption. Note that *STEREO* has a different viewpoint from satellites operated at Earth-centered orbits, such as *TRACE* and *Hinode*. (*b*) The area enclosed by the rectangle in panel *a* is enlarged and displayed in detail. The dark filament, which is marked by white arrows, can be seen to slowly rotate counterclockwise about its relatively fixed northern end. The rotation angle about the northern end is approximately 17°. (*c*) *GOES* X-ray flux at 1–8 Å (0.5–4 Å), shown with the dotted (solid) line. The onset of a B2 flare at 05:03 UT marks the beginning of the dynamic stage of the eruption. [*See the electronic edition of the Journal for a color version of this figure.*]

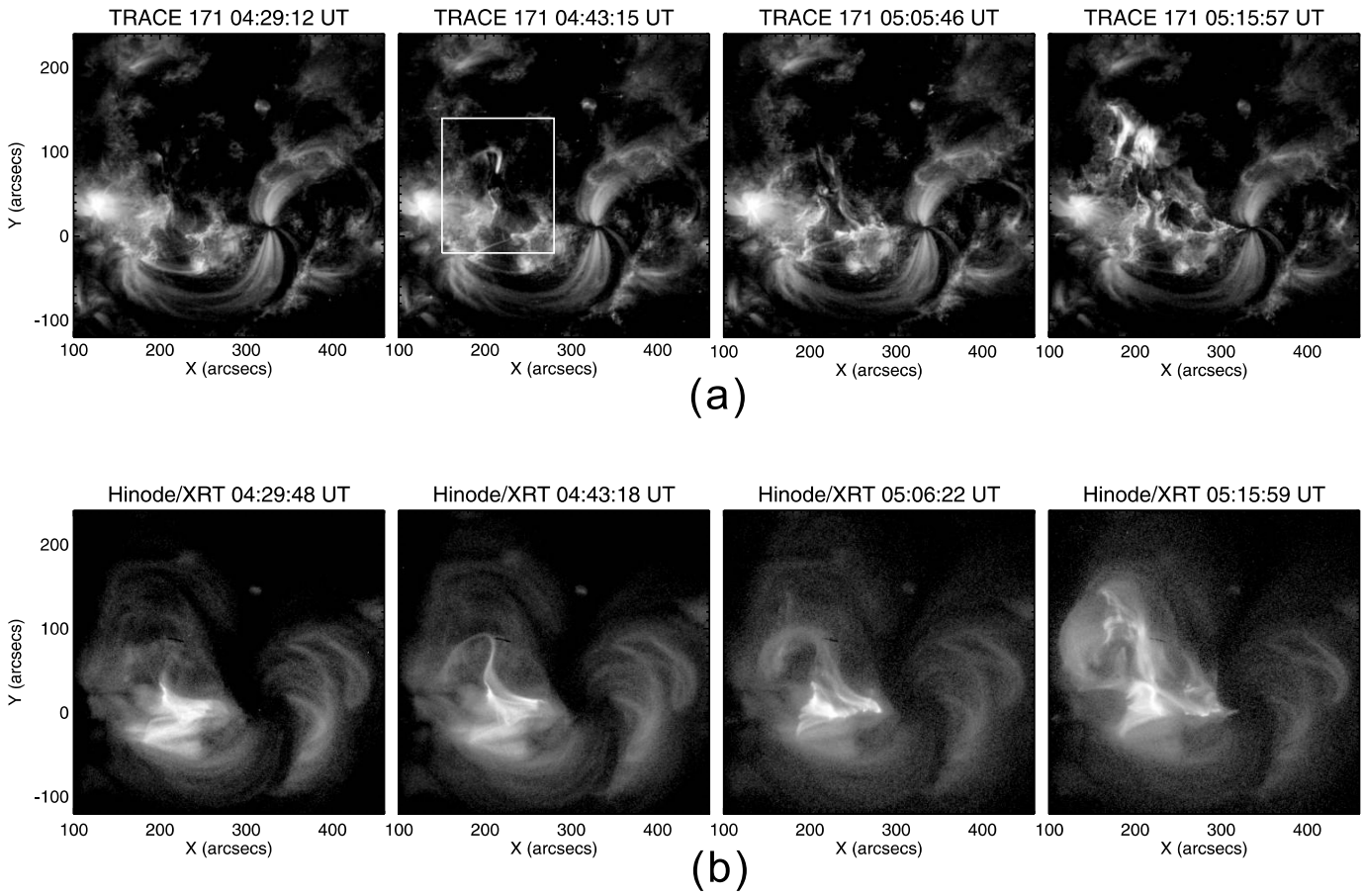

FIG. 3.—(*a*) Partial eruption observed in *TRACE* 171 Å images. (*b*) Corresponding *Hinode* XRT images. The area enclosed by the rectangle in the second *TRACE* image is enlarged and displayed in Fig. 4. [*See the electronic edition of the Journal for both a color version of this figure and mpeg animations for the TRACE and XRT images*.]

evolution (§ 2.2). The deviation of the filament spine from the original north-south orientation of the filament suggests that it is undergoing slow kinking motions. Fast kinking motions, recorded by the *TRACE* 171 Å filter, start at about 05:00 UT (§ 2.2), coincident with the onset of a *GOES* class B2 flare (Fig. 2*c*). The rotation of the filament is a signature of increasing writhe, and this provides a lower limit to how much the filament is kinked before the kink instability sets in.

2.2. *Sigmoid Transformation*

Figure 3 shows the evolution of the sigmoid, which first appeared about half an hour prior to the onset of the flare. More details are revealed in Figure 4. At 04:29:48 UT, a diffuse sigmoidal structure was visible in the SXR (Fig. 3*b*), with no counterpart in the EUV (04:29:12 UT; Fig. 3*a*). At about 04:35 UT (Fig. 4*a*), a bright ribbon-like structure appeared to thread beneath the midpoint of the dark filament in the *TRACE* 171 Å image, similar to the *STEREO* EUVI image at 04:34 UT (Fig. 2*b*). The ribbon arched toward the northern end of the filament and at 04:43:15 UT developed into the northern elbow of an inverse S–shaped sigmoid (Figs. 3*a* and 4*b*; see also Sterling et al. 2007). At this time the sigmoidal loop was sharply defined in the *Hinode* XRT data (04:43:18 UT; Fig. 3*b*), but its southern elbow was not visible in the *TRACE* 171 Å image until minutes later (Fig. 4*c*). The observation implies that the sigmoid was composed of two separate loops, as suggested by some authors (e.g., Moore et al. 2001), although it appears to be a single continuous structure in the SXR, probably due to the lower resolution and the broadband nature of the SXR data. At 05:01:41 UT, the EUV sigmoid still appeared to be "broken" at the crossing with the filament, for which two explanations are possible: (1) at the central portion of the sigmoid, there was a lack of emission within the temperature range of the 171 Å filter, which is consistent with the interpretation of the sigmoid as two separate loops, or (2) the dark filament lay above the central portion of the sigmoid and blocked the EUV emission underneath, which indicates the relative spatial relationship between the filament and the sigmoid, similar to Moore's picture (Moore et al. 2001). At 05:03:25 UT (Fig. 4*d*), the EUV sigmoid appeared as a continuous loop lying above the dark filament, suggesting a "transition" of the sigmoid across the filament. A possible alternative explanation is that part of the filament had "suddenly disappeared" as a result of dynamic motions, or that it had been heated to coronal temperatures to appear in emission in the EUV, creating a false impression of a continuous sigmoidal loop. However, it is unlikely that the filament behaved so dynamically, because the southern portion reappeared in absorption 3 minutes later at 05:06:49 UT (Fig. 5*a*), once the sigmoid had lifted off slightly.

The sigmoid-to-arcade transformation was continuously recorded by the XRT (see the mpeg animation accompanying Fig. 3*b*): the central portion of the sigmoid began to rotate counterclockwise at about 05:00 UT; as the sigmoidal loop grew in thickness, the southern portion of the sigmoid, which was originally convex toward the southeast, started to curve inward; and eventually the sigmoid developed into an arch-like structure and expanded outward, with a bright, compact loop forming underneath the erupting

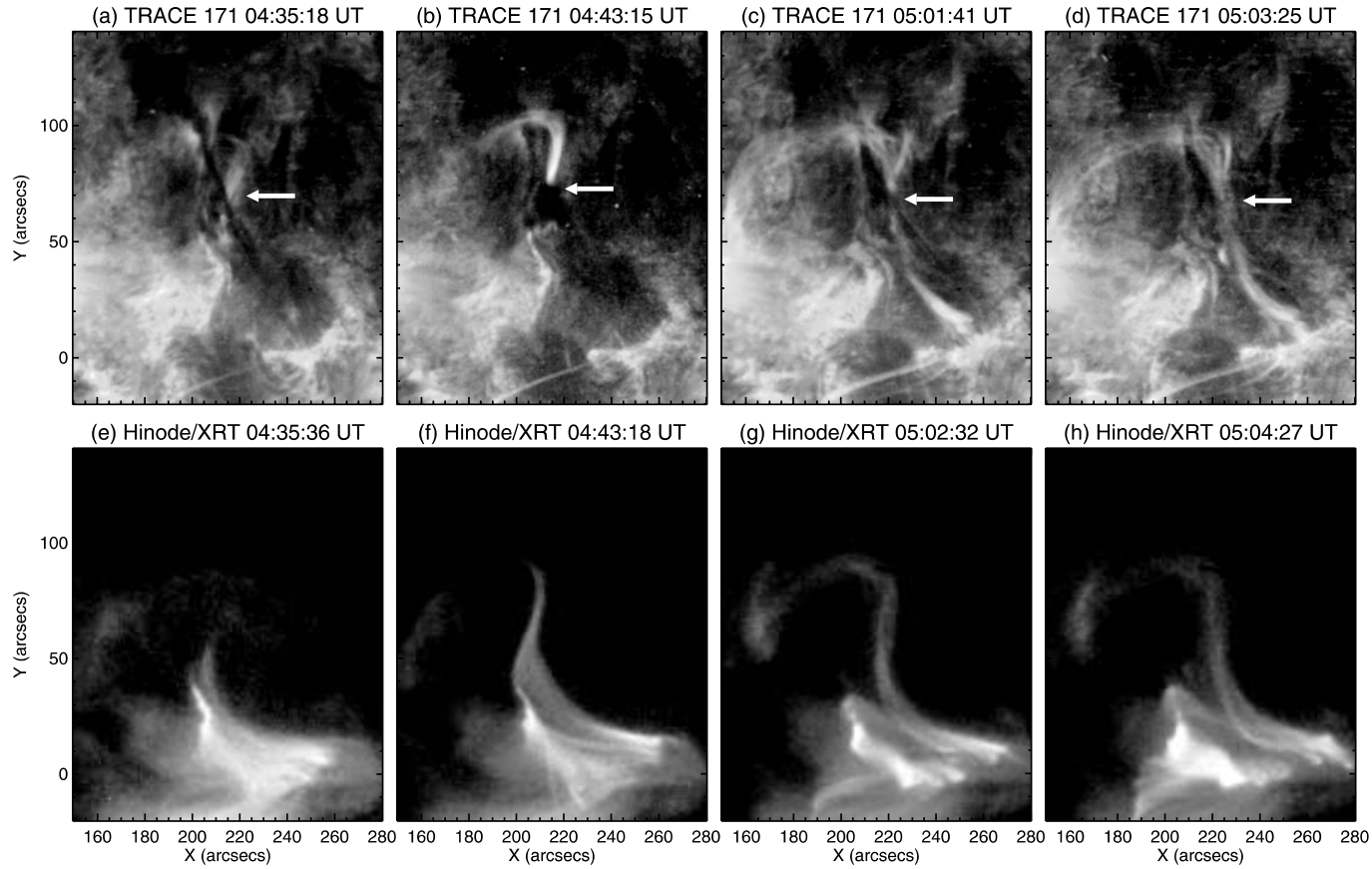

FIG. 4.—Complex spatial relationship between the transient sigmoid and the filament. White arrows mark the points where the central portion of the EUV sigmoidal loop crosses the dark filament. [*See the electronic edition of the Journal for both a color version of this figure and an mpeg animation of the TRACE images.*]

sigmoid (see the last panel in Fig. 3*b*, as well as Fig. 6*d*; see also Fig. 2 in Sterling et al. 2007), which was suggested by Sterling et al. (2007) as an evidence of internal tether-cutting.

2.3. *Partial Eruption*

Following the transformation of the sigmoid into an arched structure, the underlying filament began to quickly rotate counterclockwise and to rise with the arched sigmoid (see the *TRACE* movie accompanying Fig. 5). At 05:06:49 UT (Fig. 5*a*), it can be seen in the *TRACE* 171 Å image that the filament appeared to be composed of two strands intertwined with each other, as illustrated in the inset. At 05:10:13 UT (Fig. 5*c*), the two strands began to untangle, with one of them rotating counterclockwise. EUV brightenings were observed at the approximate separation location of the two strands, presumably due to the dissipation at an internal current sheet that formed as the filament kinked and expanded upward (Gilbert et al. 2001; Gibson & Fan 2006a). The separation of the two filament strands was illuminated by the EUV brightening. With its subtended angle increasing at a speed of approximately 10° per minute (Figs. 5*d*–5*f*), the brightening probably represents the emission from heated filament material at the separation location.

2.4. *Remaining Sigmoidal Structure*

As the upper, rotating filament strand erupted, the lower, remaining strand appeared to be heated. With the heated material moving northward along an arched direction, an inverse S–shaped dark structure was displayed in the *TRACE* 171 Å images (delineated by white dotted lines in Figs. 6*a*–6*b*). Surrounded by a hot sheath, its northern elbow became increasingly convex northwestward (Fig. 6*b*). A sigmoidal structure was also observed in the corresponding XRT images (Figs. 6*d*–6*e*) that was roughly cospatial with and similar in shape to its EUV counterpart. The original erupting sigmoid that developed into the arch-like structure can still be seen as an expanding bright shell above the sigmoidal structure that is left behind (Figs. 6*d*–6*e*).

At about 05:30 UT, an northwestward ejection from the northern elbow of the remaining sigmoidal structure can be seen in both the *TRACE* and XRT data (marked by white arrows in Figs. 6*b* and 6*e*). The ejection seemed to disrupt the remaining sigmoidal structure. As a result, it became invisible in the *TRACE* images at about 06:00 UT. The corresponding sigmoidal structure in the XRT images also dimmed at about 06:30 UT. Multiple brightening postflare loops appeared in both the *TRACE* and XRT images. The loop orientation in the SXR had a dominant east-west component, more or less normal to the north-south–oriented neutral line. In addition to these potential-like loops, there are highly sheared loops in the EUV, oriented northeast-southwest, that are invisible in the SXR.

3. DISCUSSION AND CONCLUSIONS

To summarize, the kinking motions of the filament studied here are signified by the observed rotation of the filament spine as the filament is viewed from above. The filament experiences two distinct stages of eruption in terms of the rotation speed of the filament spine: i.e., a quiescent stage with slow rotation, followed by a dynamic stage with rapid rotation. In the earlier, quiescent stage, the filament spine rotates counterclockwise quasi-statically about the relatively fixed northern end for at least an hour. A SXR sigmoid is sharply defined 15 minutes prior to the dynamic stage. Its

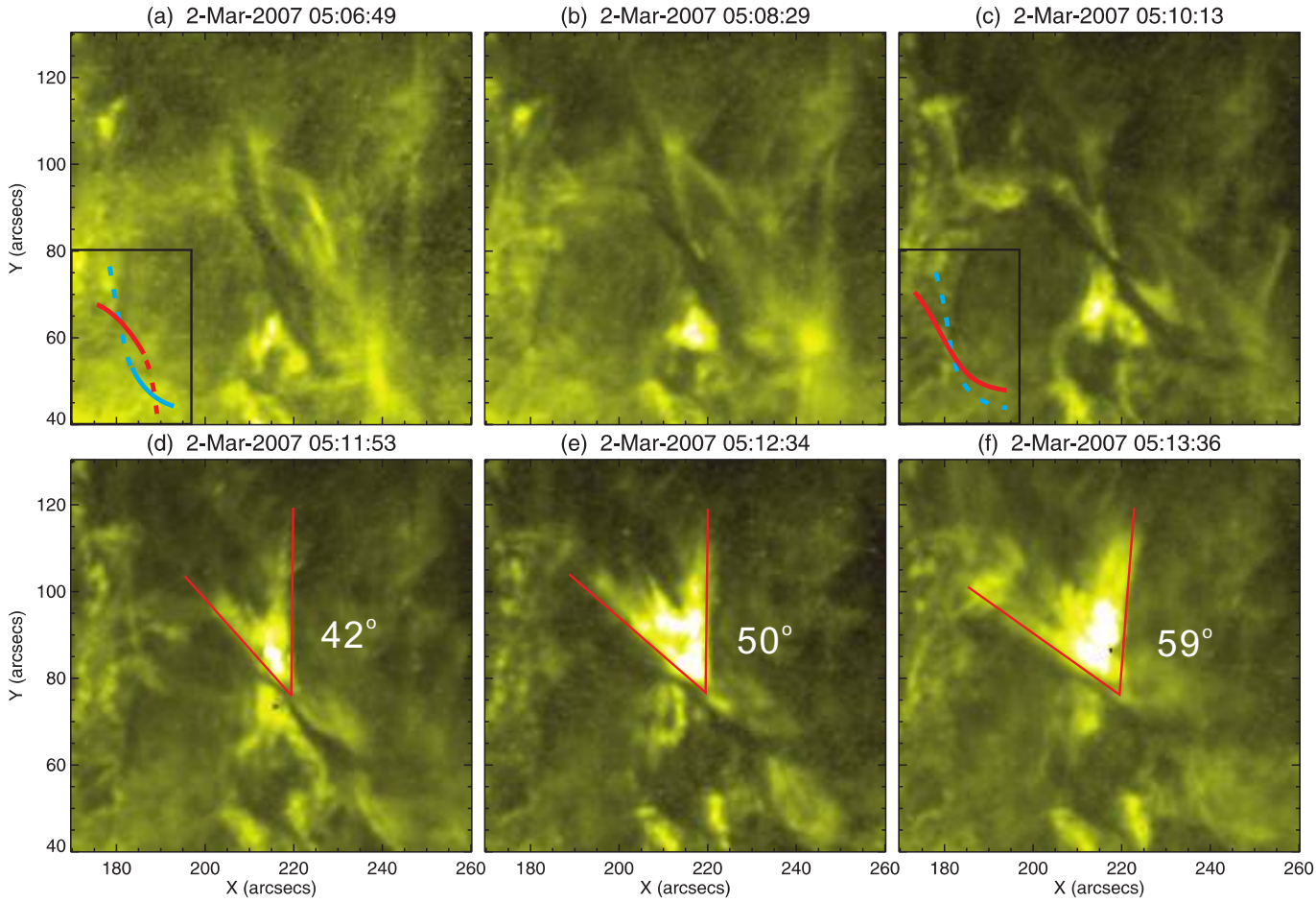

FIG. 5.—Unraveling of two filament strands initially intertwined with each other, as illustrated by the insets. The strands depicted as solid lines represent those portions of the filament that lie above the associated portions depicted by dashed lines. The separation of the two filament strands was illuminated by the EUV brightening, whose subtended angle increased at a speed of approximately 10° per minute. [*This figure is available as an mpeg animation in the electronic edition of the Journal.*]

counterpart in the EUV, however, appears to be composed of two separate loops, with the northern elbow becoming visible first, then the southern elbow. The EUV sigmoid is discontinuous at the projected crossing with the dark filament. At the onset of the dynamic stage, the EUV sigmoid appears as a single continuous structure lying above the filament, which marks the onset of a *GOES* class B2 flare and the initiation of the sigmoid-to-arcade transformation. During the dynamic stage, the filament is separated into two parts: the escaping portion rapidly rotates counterclockwise about its center and erupts with the expanding sigmoid, and the remaining portion arches northward and forms an inverse S–shaped structure.

The quasi-static kinking motions are observed before there is any heating or flaring in the EUV or the SXR (§ 2.1), which suggests that the accumulation of helicity plays an important role in initiating the eruption. Sterling et al. (2007), however, reported significant flux cancellation prior to the eruption at the neutral line associated with the eruptive filament. On the basis of other features observed in the SXR, i.e., the sigmoid-to-arcade transformation and the compact loops formed underneath the erupting sigmoid, they suggested that the eruption could also be driven by reconnection beneath the filament within the sheared core field; i.e., internal tether-cutting (Moore et al. 2001).

Other features observed in the event studied here seem to be consistent with an eruption driven by the kink instability: e.g., the fast kinking of the filament spine, the sigmoidal loop lying above the filament at the eruption onset, the separation of the filament, and the remaining sigmoidal structure. Most of these features are demonstrated in the 3D simulations performed by Fan and Gibson (Fan 2005; Gibson & Fan 2006a, 2006b), in which the kink instability is instrumental in initiating the eruption. In their simulations, a twisted magnetic flux tube emerges slowly into the corona previously occupied by a potential arcade. The evolution of the flux tube is characterized by a quasi-static kinking phase that precedes the loss of confinement and the partial eruption of the tube, which undergoes rapid kinking motions, with a sigmoidal structure left behind.

In Fan's model (Fan 2005), the accumulation of helicity in the corona, which leads to the onset of the kink instability, is accomplished by flux emergence. However, helicity can also build up by shearing motions (e.g., Amari et al. 2003a), flux cancellation (e.g., van Ballegooijen & Martens 1989; Amari et al. 2000; Linker et al. 2001), and turbulent diffusion (e.g., Mackay & van Ballegooijen 2006a, 2006b; Amari et al. 2003b). In particular, flux cancellation, which may be interpreted as the emergence of a subphotospheric flux rope or as a combination of photospheric shearing flows and the emergence or submergence of opposite polarities, can lead to the creation of a coronal flux rope, as well as to its eventual destabilization and eruption (e.g., Linker et al. 2001). Thus, the flux cancellation observed by Sterling et al. (2007), which was ongoing for at least 6 hr prior to the eruption, could contribute to the buildup of twist within the flux rope that holds the filament at its base. About 1 hr prior to the eruption, as the twist builds up, the filament begins to exhibit quasi-static kinking motions. At the eruption

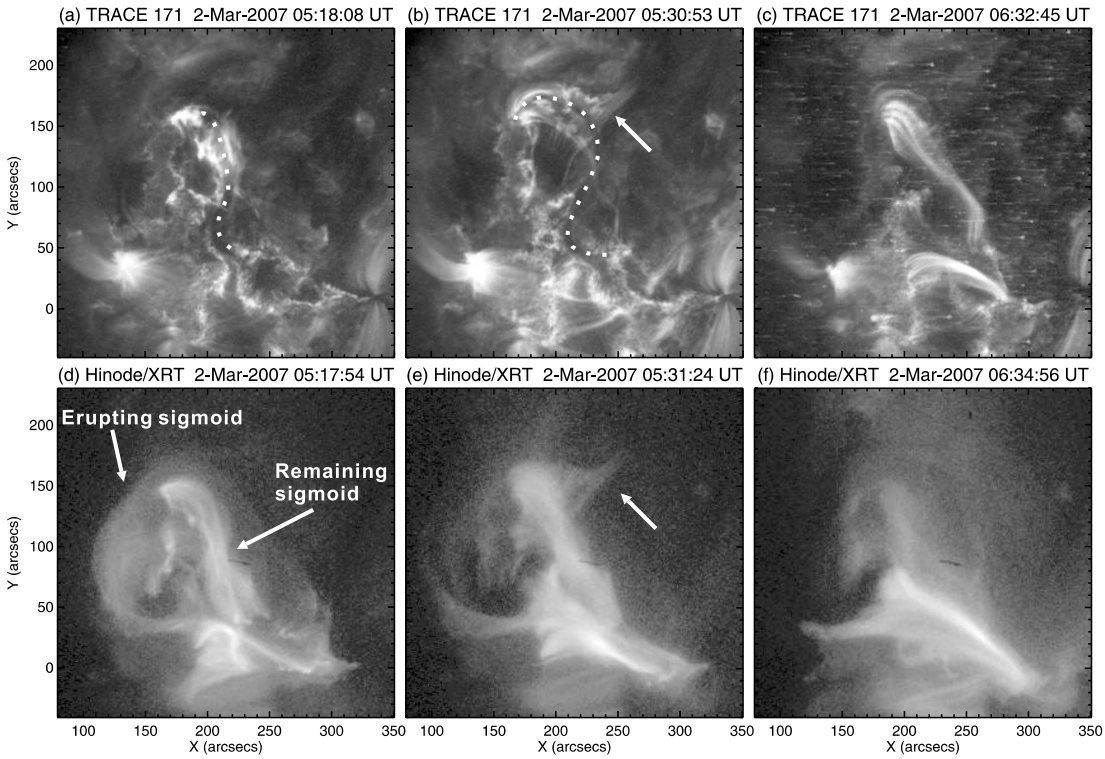

FIG. 6.—Remaining sigmoidal structure. In the *TRACE* 171 Å images (*top*), the remaining portion of the filament developed into a dark, inverse S–shaped structure (*white dotted lines*), with its northern portion surrounded by a hot, semitransparent sheath. It is cospatial with a sigmoidal structure in the corresponding XRT images (*bottom*). The original sigmoid can be seen as an expanding bright shell in the XRT data. A secondary ejection from the northern elbow of the remaining sigmoidal structure is marked by the white arrows in panels *b* and *e*. [*See the electronic edition of the Journal for a color version of this figure*.]

onset, the twist reaches the instability threshold, instigating the kink instability, with the filament showing the consequent rapid kinking motions (see simulation by Fan 2005). In general, both internal tether-cutting and external tether-cutting (see the review by Moore & Sterling 2006) could involve the onset of the kink instability as the twist within the flux rope, which is created by reconnections of sheared arcades prior to or during the eruption, reaches the instability threshold.

The evolution of the sigmoid in relation to the filament can be understood within the framework of Fan and Gibson's simulations. It has been suggested that hot sigmoidal loops observed in EUV or SXR emissions are the manifestations of sheared field with enhanced current density (e.g., Kliem et al. 2004; Gibson et al. 2004). Reconnection and associated dissipative heating can occur in current sheets along separatrix surfaces where distinct flux systems contact one another. In particular, a bald-patch–associated separatrix surface (BPSS) with a sigmoidal shape can be formed where the dipped portion of winding field lines tangentially grazes the photosphere along the polarity inversion line (Titov & Démoulin 1999; Low & Berger 2003). In this configuration the filament lies within and above the BPSS, with the filament aligned with the central portion of the BPSS along the polarity inversion line. Field lines in the BPSS have a high, arched end and a low, dipped end (see magenta lines in Fig. 2*e* of Gibson & Fan 2006b). Opposing upper portions of BPSS field lines can reconnect when they are squeezed together due to the kinking motion of the flux rope (see Fig. 6*c* in Gibson & Fan 2006b).

The reconnection is similar to the internal tether-cutting in the sense that it occurs between two oppositely curved J-shaped field lines. But now that it is driven by the kinking motions of the flux rope, there are three important differences from the internal tether-cutting model. *First*, as the flux rope kinks and expands upward, a vertical current sheet is formed within the flux rope (Gibson & Fan 2006a). The dissipation at the internal current sheet breaks the flux rope in two, which could account for the separation of the filament and the EUV brightening at the separation location in our observations. *Second*, the reconnection occurs between higher arched portions of two elbow-like field lines, as opposed to the reconnection of lower dipped portions by internal tether-cutting, which results in a higher reconnection location, probably within, or even above, the filament. If the reconnection occurs above the filament, the reconnected lines above the reconnection site could be observed as an EUV sigmoidal loop arching over the filament if the field lines are heated to coronal temperatures via the reconnection. In Gibson & Fan (2006a), the reconnection that breaks the flux rope into two starts to occur at $t = 90$, right after the flux emergence is stopped at $t = 86$ (see Fig. 3 in Gibson & Fan 2006a). This is consistent with the observation studied here, as the "broken" EUV sigmoid appears to be continuous at 05:03 UT, coincident with the onset of the flare and the dynamic phase of the eruption. *Third*, the reconnected lines below the reconnection site form a sigmoidal structure underneath, as opposed to the low-lying compact loops formed by internal tether-cutting. Thus, in the above scenario, the filament would not necessarily be totally expelled with the expanding sigmoid, which may shed some light on the mystery that some filaments apparently survive the sigmoidal-to-arcade transformation (Pevtsov 2002; Gibson et al. 2002).

The observation that the erupting part of the filament rotates counterclockwise while the sigmoid (in both the EUV and the SXR) exhibits an inverse S shape (indicating negative helicity) is in line with the very recent results of Green et al. (2007), who find the same relationship between the rotating filament and the sigmoid shape (counterclockwise rotation is associated with the inverse S–shaped sigmoids, whereas clockwise rotation is associated

with the forward S−shaped sigmoids) in all of the events they studied. This relationship is in agreement with the implications of both the model proposed by Titov & Démoulin (1999) and the tether-cutting model (Moore et al. 2001).

The observations presented here suggest that the kink instability and internal tether-cutting may work together in initiating the eruption, as the two mechanisms are not mutually exclusive (see also Sterling et al. 2007; Williams et al. 2005). As a result, magnetic reconnections may occur above, within, or beneath the filament. (1) Coincident with the onset of a small flare, the transition of the EUV sigmoid from a discontinuous to a continuous structure lying above the filament suggests reconnection above the filament, driven by the kinking motions. (2) The separation of the filament into two, the EUV brightening at the separation point, and the remaining sigmoid structure suggest that reconnection occurs within the filament, at the internal current sheet formed due to the kinking motions. (3) Reconnection may occur beneath the filament to form the low-lying compact loops observed by Sterling et al. (2007).

We would like to thank Tibor Török for an extremely thoughtful and useful review of the paper. We also thank the *STEREO* SECCHI, *Hinode* XRT, and *TRACE* consortia for their data. *STEREO* is a project of NASA. *Hinode* is a Japanese mission developed and launched by ISAS/JAXA, with NAOJ as domestic partner and NASA and STFC (UK) as international partners. It is operated by these agencies in cooperation with ESA and the NSC (Norway). *TRACE* is operated jointly out of Goddard Space Flight Center by scientists from the University of Chicago, Montana State University, LMSAL, and the Harvard-Smithsonian Center for Astrophysics. This work was supported by SHINE under NSF grant ATM-0353345.

REFERENCES

Alexander, D., Liu, R., & Gilbert, H. R. 2006, ApJ, 653, 719
Amari, T., Luciani, J. F., Aly, J. J., Mikic, Z., & Linker, J. 2003a, ApJ, 585, 1073
———. 2003b, ApJ, 595, 1231
Amari, T., Luciani, J. F., Mikic, Z., & Linker, J. 2000, ApJ, 529, L49
Berger, M. A. 1998, in IAU Colloq. 167, New Perspectives on Solar Prominences, ed. D. F. Webb, B. Schmieder, & D. M. Rust (ASP Conf. Ser. 150; San Francisco: ASP), 102
Berger, M. A., & Prior, C. 2006, J. Phys. A, 39, 8321
Fan, Y. 2005, ApJ, 630, 543
Gibson, S. E., & Fan, Y. 2006a, ApJ, 637, L65
———. 2006b, J. Geophys. Res., 111, A12103
Gibson, S. E., Fan, Y., Mandrini, C., Fisher, G., & Demoulin, P. 2004, ApJ, 617, 600
Gibson, S. E., et al. 2002, ApJ, 574, 1021
Gilbert, H. R., Alexander, D., & Liu, R. 2007, Sol. Phys., 245, 287
Gilbert, H. R., Holzer, T. E., & Burkepile, J. T. 2001, ApJ, 549, 1221
Gilbert, H. R., Holzer, T. E., Burkepile, J. T., & Hundhausen, A. J. 2000, ApJ, 537, 503
Golub, L., et al. 2007, Sol. Phys., 243, 63
Green, L. M., Kliem, B., Török, T., van Driel-Gesztelyi, L., & Attrill, G. D. R. 2007, Sol. Phys., 246, 365
Handy, B. N., et al. 1999, Sol. Phys., 187, 229
Kliem, B., Titov, V. S., & Török, T. 2004, A&A, 413, L23
Linker, J. A., Lionello, R., Mikić, Z., & Amari, T. 2001, J. Geophys. Res., 106, 25165
Liu, R., Alexander, D., & Gilbert, H. R. 2007, ApJ, 661, 1260
Low, B. C., & Berger, M. A. 2003, ApJ, 589, 644
Mackay, D. H., & van Ballegooijen, A. A. 2006a, ApJ, 641, 577
———. 2006b, ApJ, 642, 1193
Moore, R. L., & LaBonte, B. J. 1980, in IAU Symp. 91, Solar and Interplanetary Dynamics, ed. M. Dryer & E. Tandberg-Hanssen (Dordrecht: Reidel), 207
Moore, R. L., & Sterling, A. C. 2006, in Solar Eruptions and Energetic Particles, ed. N. Gopalswamy, R. Mewaldt, & J. Torsti (Geophys. Monogr. 165; Washington: AGU), 43
Moore, R. L., Sterling, A. C., Hudson, H. S., & Lemen, J. R. 2001, ApJ, 552, 833
Pevtsov, A. A. 2002, Sol. Phys., 207, 111
Romano, P., Contarino, L., & Zuccarello, F. 2003, Sol. Phys., 218, 137
Rust, D. M., & Kumar, A. 1994, Sol. Phys., 155, 69
———. 1996, ApJ, 464, L199
Rust, D. M., & LaBonte, B. J. 2005, ApJ, 622, L69
Sterling, A. C., Hudson, H. S., Thompson, B. J., & Zarro, D. M. 2000, ApJ, 532, 628
Sterling, A. C., et al. 2007, PASJ, 59, 823
Titov, V. S., & Démoulin, P. 1999, A&A, 351, 707
Török, T., & Kliem, B. 2005, ApJ, 630, L97
van Ballegooijen, A. A., & Martens, P. C. H. 1989, ApJ, 343, 971
Williams, D. R., Török, T., Démoulin, P., van Driel-Gesztelyi, L., & Kliem, B. 2005, ApJ, 628, L163
Wuelser, J.-P., et al. 2004, Proc. SPIE, 5171, 111